Desalination and Water Treatment
www.deswater.com

doi: 10.1080/19443994.2015.1110838

57 (2016) 20889–20903
September

Taylor & Francis
Taylor & Francis Group

Characterization of peat samples collected from Brunei Darussalam and their evaluation as potential adsorbents for Cu(II) removal from aqueous solution

Tasneem Zehra[a], Linda B.L. Lim[a,*], Namal Priyantha[b,c]

[a]*Faculty of Science, Department of Chemistry, Universiti Brunei Darussalam, Jalan Tungku Link, Gadong, Negara Brunei Darussalam, email: if_tz@hotmail.com (T. Zehra), Tel. +673 8748010; email: linda.lim@ubd.edu.bn (L.B.L. Lim)*
[b]*Faculty of Science, Department of Chemistry, University of Peradeniya, Peradeniya, Sri Lanka, email: namal.priyantha@yahoo.com*
[c]*Postgraduate Institute of Studies, University of Peradeniya, Peradeniya, Sri Lanka*

Received 13 February 2015; Accepted 18 October 2015

ABSTRACT

In this study, the peat samples from two different sites of Brunei Darussalam (Mumong and Panaga) were investigated. The peats were found to be acidic in nature containing 66–75% organic matter. Thermogravimetric analysis revealed their thermal stability up to 500°C, while scanning electron microscopy, Fourier transform infrared spectroscopy, and X-ray fluorescence provided information on the modes of interaction of Cu(II) ions with peat through complexation and ion-exchange mechanisms. Further, the extent of removal of Cu (II) ions from aqueous solution investigated under different experimental conditions revealed that the optimum values for shaking time and medium pH were 3.0 h and 5.5, respectively. Equilibrium adsorption data fitted to the Langmuir, Freundlich, Temkin, Dubinin–Radushkevich (D–R), Redlich–Peterson (R–P), and Sips isotherm models indicated that adsorption of Cu(II) ions on peat obeyed the Sips model with an average adsorption capacity of 16.5 and 14.6 mg g^{-1} for the Mumong and Panaga peat, respectively. Application of the pseudo-first-order, pseudo-second-order, Elovich, Boyd, and intraparticle diffusion models to evaluate the kinetics of the adsorption process led to the validity of the pseudo-second-order and intraparticle diffusion models to explain the adsorption of Cu(II) ions on the selected peat samples.

Keywords: Peat; Adsorption; Cu(II) removal; Equilibrium isotherm; Kinetics; XRF

1. Introduction

Peat, a kind of soil containing 50–95% organic substances, is formed by partial decomposition of vegetation and animal constituents under wet conditions. Peatlands are in all continents. Tropical peatlands are located in South-East Asia, Africa, the Caribbean, Central and South America. South-East Asia's peatlands cover 69% of the tropical peatland and makes 11% of the global peatland area [1]. Studies have proven that peat, which consists of various functional groups including lignin phenols [2], is an efficient adsorbent for removing pollutants from wastewater [3–6]. In this study, peat samples collected from two different sites (Mumong and Panaga) of the Belait district in Brunei Darussalam were investigated for their characteristics and adsorption properties.

Heavy metal ions, recognized as ecotoxicological hazardous substances [7], are not biodegradable and

---

*Corresponding author.

can accumulate in living tissues. Among many conventional methods that have been used for removing metal ions and their compounds from industrial effluents, adsorption techniques are the most widely used [8]. Abundant natural materials [9,10], agricultural waste materials [11,12], ion-exchange resins [13–15] have been used as potential inexpensive adsorbents for heavy metal removal. Adsorption, although highly effective, is a complex process consisting of several mechanisms that differ according to the metal species in solution and types of adsorbents.

Copper is used extensively in many industries, such as refineries, paper and pulp, fertilizer, mining, and plating baths. Its removal by low-cost adsorbents has been studied widely [16–22]. In the present work, the usefulness of peat samples collected from two different sites has been investigated for the removal of copper ions from aqueous solutions. Batch experiments were designed to study the influence of contact time, pH, and metal concentration on the adsorption process. Modeling of adsorption processes is important for the prediction of metal distribution between the aqueous solution and the solid surface of the adsorbent. Its application helps to design adsorption treatment units as well as to evaluate the fate of heavy metal ions and their compounds in the natural environment. Six isotherm models (Langmuir, Freundlich, Temkin, Dubinin–Radushkevich, Redlich–Peterson, and Sips models) were used in this study to predict the best-fit model for the adsorption equilibrium data. Surface morphology was analyzed using scanning electron microscopy (SEM). The change in elemental composition of peat during adsorption was determined using X-ray fluorescence (XRF) spectroscopy. Fourier transform infrared (FTIR) spectroscopy was carried out to determine the main functional groups present in peat that might be involved in metal uptake.

2. Materials and methods

Copper nitrate, ($Cu(NO_3)_2{\cdot}3H_2O$) (Sigma–Aldrich), was used for the preparation of 1,000 mg L^{-1} stock solution by dissolving the required amount in double-distilled water. Other concentrations of Cu(II) were obtained by appropriate dilution of the stock solution. The pH of Cu(II) solutions was adjusted using concentrated NaOH and HNO_3 solutions. Flame atomic absorption spectrometer (Shimadzu AA-6701F) was used to record absorbance measurements to determine the concentration of Cu(II) in all solutions. Stuart orbital shaker used for agitation of solutions was set at 250 rpm.

2.1. Sample collection and preparation

Peat samples were collected from two different sites of Brunei Darussalam, namely Mumong and Panaga. The peat samples collected from different sites were dried in oven at 60˚C, followed by sieving to collect particles of diameter 350–850 μm. Sieved samples were used for all experiments.

2.2. Characterization of peat

The bulk density, pH, ash content, total phenolics, moisture content, and crude fiber of each peat sample were determined using standard procedure. CHNS analyses of samples were performed using the Elementar Vario Micro Cube analyzer. Functional group characterization of peat before and after treatment with Cu(II) was carried out using FTIR spectrophotometer (Shimadzu Model IRPrestige-21). XRF PANalyticalAxios^{max} was used for elemental analysis and SEM images of peat samples were obtained using Tescan Vega XMU Scanning electron microscope (SEM). Thermogravimetric analysis (TGA) curves were recorded using thermogravimetric analyzer (Scino Instruments Model STA N-650).

2.3. Batch adsorption experiments

Batch experiments were carried out by mixing 0.10 g of adsorbent with 50.0 mL of metal solution of known concentration for all experiments. Effect of contact time was investigated by agitating mixtures followed by filtration at predetermined time intervals. Effects of initial metal concentration and pH on the extent of Cu(II) removal were also investigated. All experiments were carried out in duplicate, and the average results were reported. Eq. (1) was used to calculate the amount of metal adsorbed per gram of adsorbent, q_e (mg g^{-1}):

$$q_e = \frac{(C_i - C_e)V}{m} \tag{1}$$

where C_i is the initial metal concentration (mg L^{-1}), C_e is the equilibrium metal concentration (mg L^{-1}), V is the volume of metal solution used (L), and m is the mass of adsorbent used (g). The percentage removal of the Cu(II) is represented by Eq. (2) as follows:

$$\%\ \text{Removal} = \frac{(C_i - C_e) \times 100}{C_i} \tag{2}$$

3. Results and discussion

3.1. Characterization of peat

Bulk density is an indicator of soil compaction; the higher the bulk density, the lower the soil prosperity and compaction. In this study, peat from Panaga is twice as dense as that from Mumong (Table 1). High bulk density, from 0.10 to 0.32 g cm^{-3}, appears to be a general feature of most tropical peats under natural conditions due to the effect of climate, height of water table, and oxidation. On the basis of results obtained for bulk density of peat samples, peat collected from Mumong and Panaga sites can be classified as Hemic (intermediate in degree of decomposition) and Sapric (highly decomposed), respectively [23].

Although peat mainly consists of organic matter, it does contain various inorganic materials resulting from decomposition and sediment loading in peatlands. The ash content of both peat samples falls within the range of 10–50%, characteristic of decomposed peat. High value of ash is an indication of high amount of mineral soil in peat. The ash or inorganic content from less than 1 to 65% has been reported for tropical peat [24]. The peat samples collected from Brunei are found to be acidic in nature, with point of zero charge (pH_{pzc}) for Mumong and Panaga being at pH 4.5 and 2.0, respectively [25]. Similar results have been reported for peat of the Borneo region [26,27].

C, H, O, N, and S are five basic elements of peat. Generally, peat has elemental composition which is between that of wood and coal. Low-decomposed peat resembles wood, while high-decomposed peat with that of the lignite. The composition of peat varies depending on age, nature of original vegetation, climate, and other environmental factors. The H/C ratio has been associated with degree of aromaticity. Lower the ratio, greater will be aromatic compounds in peat. On the other hand, the C/N ratio indicates microbial activities. It has been reported that an increase in the C/N ratios indicates decrease in peat decomposition and vice versa [28]. Although H/C ratio value is similar for both peat samples (Table 2) suggesting both have similar degree of aromatic components, Panaga peat has a significantly lower C/N ratio making it more decomposed peat.

The phenolic contents for both the peat samples are found to be 0.695 and 0.627 mg GAE g^{-1} for the Mumong and Panaga peat, respectively, which are very low compared to that of the peat bog of Hokkaido Island, Japan, ranging from 1.6 to 19 mg g^{-1} [29] and of peat collected from a pristine site in Brunei Darussalam with values ranging from 13 to 28 mg g^{-1} [30]. Phenolics in peat have a potential inhibitory effect on microbial and enzyme activates involved in organic matter decomposition. Thus, low %C as reported in CHNS above may be a result of high decomposition of peat due to low presence of phenolics.

3.2. Thermal properties of peat

Three major mass losses identified by TGA curves are water evaporation, combustion of volatile matter (pyrolysis process increases and hemicellulose and cellulose decompose into gases such as CO_2, CO, CH_4 leading to the formation of carbonaceous char), and combustion of charcoal matter (self-combustion with the rapid mass loss due to the presence of large amount of lignin in the peat soil) [31]. The thermogram obtained for peat samples in Fig. 1 shows the three major regions as described earlier. The mass loss for each region for peat samples, given as a percentage in Table 3, indicates the highest loss in the middle region.

3.3. SEM, FTIR, and XRF analyses

SEM images in Fig. 2 show that the surface of peat samples is very uneven and heterogeneous in nature with pores or cavities. Some threadlike structures observed could be the fibers present in peat samples.

Analysis of FTIR spectra of the Panaga and Mumong peat, before and after adsorption of Cu(II), shown in Fig. 3, reveals a number of major absorption

Table 1
Physical and chemical properties of Mumong and Panaga peat

Characteristic	Mumong	Panaga
Bulk density (g cm^{-3})	0.09	0.22
Moisture (%)	69.0	48.3
Color	Dark grayish	Dark grayish to black
pH	4.4	3.1
Ash (%)	33.6	24.8
Organic matter (OM)	66.4	75.2
Crude fiber (%)	4.49	3.71

Table 2
CHNS analysis for peat samples

Adsorbent	%C	%H	%N	%S	H/C[a]	C/N[b]
Mumong	14.18	1.80	0.34	<0.5	1.51	48.62
Panaga	13.37	1.67	1.93	1.93	1.45	8.08

[a] H/C = [(%H/1.008)/(%C/12.01)].
[b] C/N = [(%C/12.01)/(%N/14.00)].

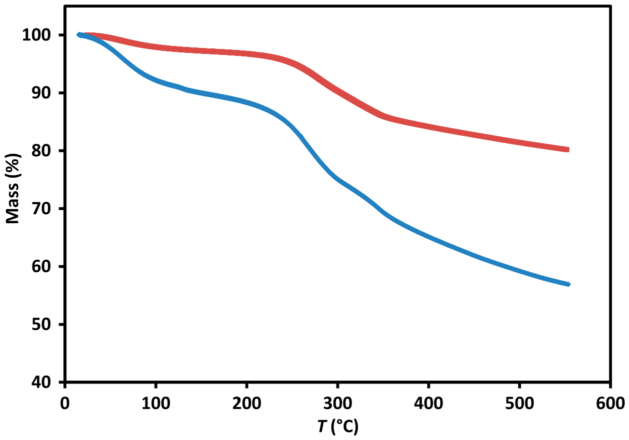

Fig. 1. Thermogram for peat samples: Mumong (■) and Panaga peat (♦).

Table 3
Percentage mass loss of the peat samples in different ranges of temperature

Temperature range (°C)	Mumong (%)	Panaga (%)
15–150	2.73	10.04
150–350	11.37	20.61
350–500	5.69	12.44
Total mass loss	19.79	43.09

bands indicating the characteristic structure of peat before and after Cu(II) adsorption. For peat samples, a strong band at 3,360 cm^{-1} indicates the presence of –NH or –OH, whereas bands in the 3,000–2,850 cm^{-1} region represent C–H groups [32,33]. Peaks at 3,360 and 1,632 cm^{-1} were observed to be shifted to 3,285 and 1,614 cm^{-1} after Cu(II) adsorption on Mumong peat; whereas in Panaga peat, intensities of peaks at 2,922, 2,852, and 1,620 cm^{-1} decreased by about 14% on average after Cu(II) adsorption. Shifts or changes of these peaks would indicate interactions between Cu (II) with functional groups on the surface of peat, as a result of adsorption, forming complexes.

Elemental analyses by XRF carried out for the Mumong and Panaga peat indicate the absence of copper before Cu(II) adsorption (Table 4). XRF spectra of peat upon treatment with Cu(II) clearly show that peat was able to adsorb Cu(II) ions (Fig. 4), supporting observations made in FTIR spectra. Decrease in the intensity of peaks associated with metallic elements suggests that ion exchange plays an important role in the removal of Cu(II) ions from aqueous solution, in addition to complexation as proposed by FTIR spectral investigation.

3.4. Optimization of contact time for Cu(II) removal

The optimum shaking time for the removal of 10 mg L^{-1} Cu(II) solution by peat collected from Mumong and Panaga sites is found to be 3.0 h for both types of peat (Fig. 5) with the Mumong peat showing a higher removal (60%) than Panaga (45%). Compared to the removal of Cu(II) by other adsorbents carried out under similar experimental conditions, adsorbents such as *Artocarpus altilis* skin and core required 3.0 and 3.5 h, respectively [34], while undisturbed pristine peat [35] and *Artocarpus odoratissimus* core [36] reached equilibrium within a much shorter time period of 2.0 h.

3.5. Effect of pH

Medium pH is one of the important parameters in adsorption studies as it influences the extent of removal of adsorbate by the adsorbent. The effect of pH was investigated within the range of pH 3–7 to avoid possible precipitation of Cu(II) as its hydroxide at higher pH values [35,36]. Fig. 6 shows the percentage removal of Cu(II) ions by the Mumong and Panaga peat at different pHs. Low removal of Cu(II) at pH 3 is attributed to competition between H_3O^+ ions with Cu(II) ions for the limited number of active sites on the adsorbent's surface [37]. An increase in the extent of removal upon the increase in solution pH is partly attributed to an increase in the negative charges on the adsorbent surface, thereby attracting the positive metal ions toward the adsorbent. Hence, the ambient pH of 5.5 was selected for further adsorption experiments. Similar findings were also reported for the adsorption of Cu(II) on breadfruit skin [34] and pristine peat [36].

3.6. Adsorption kinetics

Adsorption kinetics provides valuable information on the mechanism and reaction pathways of

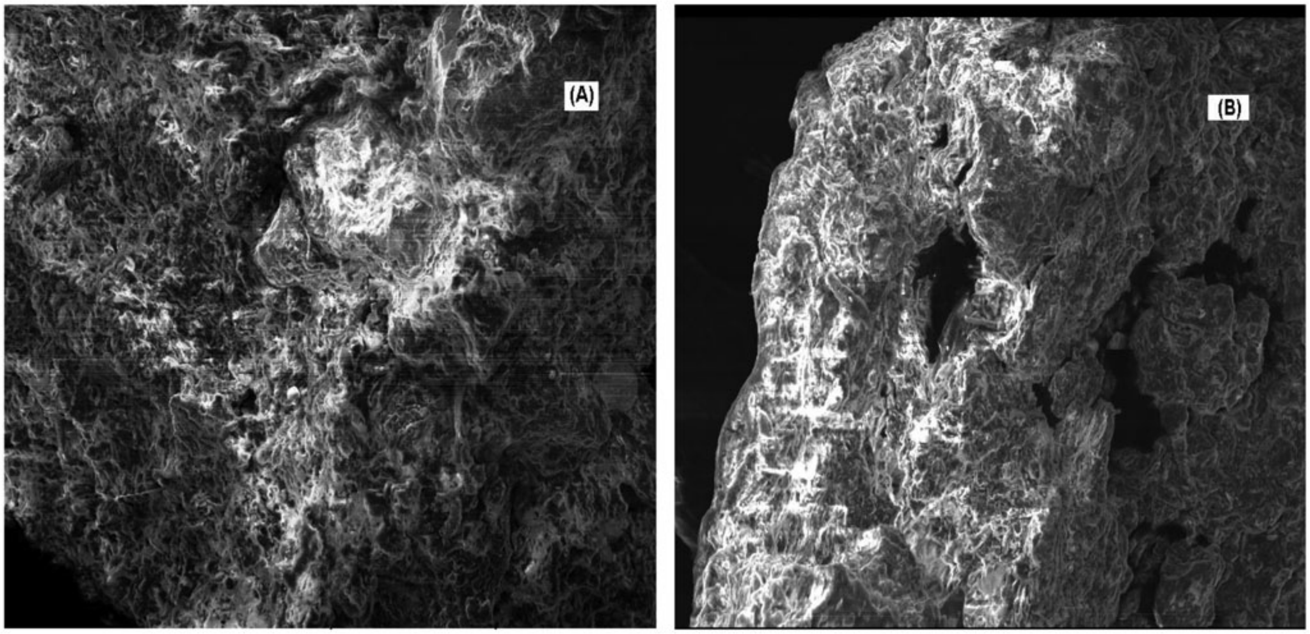

Fig. 2. SEM images of (A) Mumong peat and (B) Panaga peat.

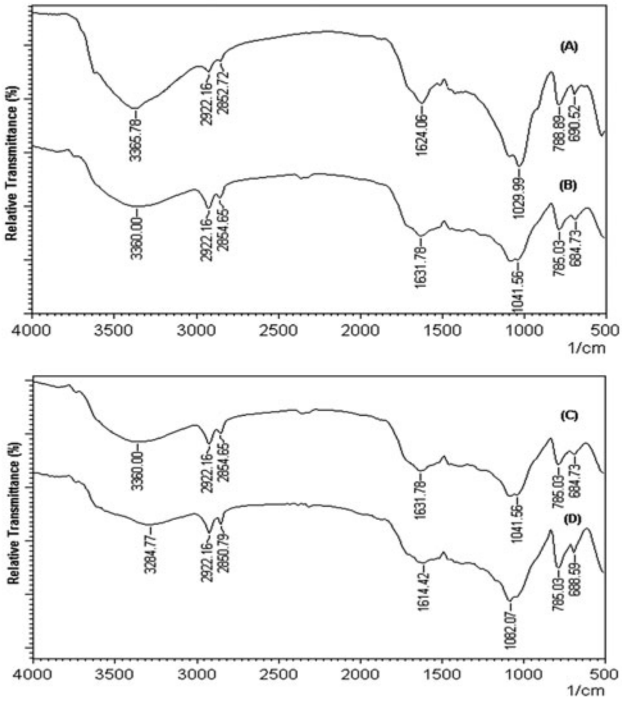

Fig. 3. FTIR spectra of peat for Panaga (A), Mumong (B), Cu-loaded Panaga (C), and Cu-loaded Mumong (D).

adsorption process. The kinetics plots for the adsorption of Cu(II) on Mumong and Panaga peat presented in Fig. 7 show the amount of Cu(II) adsorbed at different time intervals starting from 5 min until equilibrium is reached with the initial adsorbent concentration of 10.0 mg L^{-1}. It is clear from the figure that the adsorption capacity of peat gradually increases with an increase in the interaction time followed by a slow process until the equilibrium is established. At equilibrium, the adsorption capacity of Cu (II) is found to be 0.045 and 0.034 mmol g^{-1} for Mumong and Panaga peat, respectively. It has been reported that adsorption kinetics includes two steps: a fast sorption at the initial stages of contact time and then becomes slower near the equilibrium [38]. This two-step behavior is adsorption characteristics attributed to the heterogeneity of the surface binding sites with different binding affinities to metal ions result in different binding rates in a heterogeneous adsorbent [39].

Linear plots of five common models: pseudo-first order [40], pseudo-second order [41], Elovich [42], Boyd [43], and Weber–Morris intraparticle diffusion [44] evaluated for kinetics of Cu(II) adsorption are given in Fig. 8.

The linear form of the pseudo-first-order equation proposed by Lagergren is expressed as:

$$\log\left(q_{\mathrm{e}}-q_t\right)=\log q_{\mathrm{e}}-\left(\frac{k_1}{2.303}\right)t \tag{3}$$

where q_{e} and q_t are the amounts of Cu(II) adsorbed (mmol g^{-1}) at equilibrium and at time t (min),

Table 4
Percentage composition of major elements of peat samples before and after Cu(II) adsorption

Element	Mumong peat	Mumong—after adsorption	Panaga peat	Panaga—after adsorption
Ca	1.3	0.9	0.6	0.1
Cl	0.2	0.1	1.0	0.1
K	0.9	0.7	1.6	1.5
Mg	0.4	0.3	1.1	0.6
Na	0.2	0.1	0.9	0.4
P	0.3	0.2	0.1	0.1
S	1.4	0.7	6.3	6.3
Si	39.6	36.7	27.1	26.8
Cu	–	1.3	–	1.0

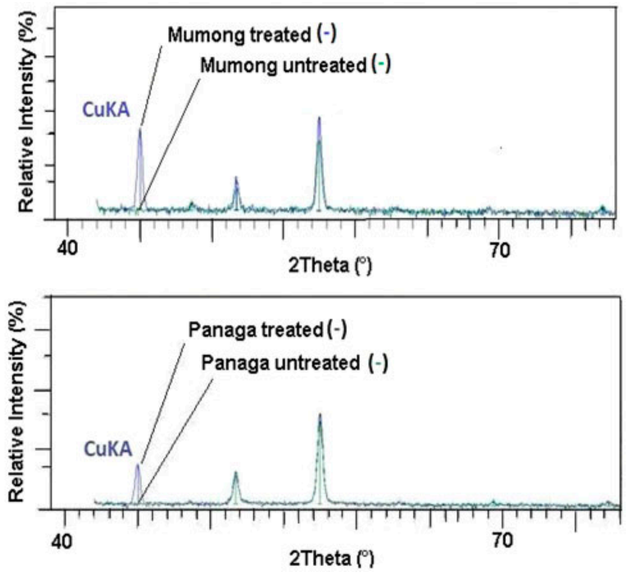

Fig. 4. XRF spectra of peat showing copper before and after adsorption: Mumong (top) and Panaga (bottom).

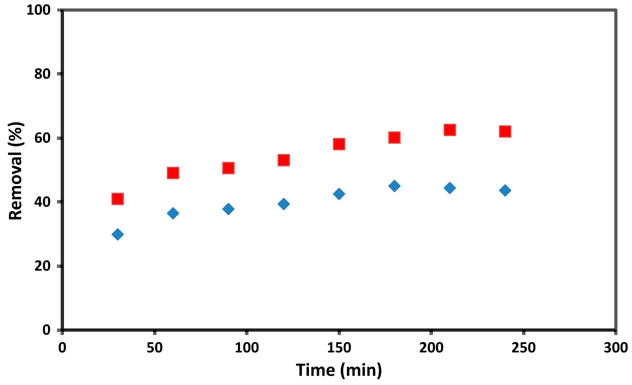

Fig. 5. Optimum shaking time for Cu(II) removal by Mumong (■) and Panaga peat (◆): concentration of metal solution: 10.0 mg L^{-1}; volume: 50.0 mL; peat: 0.10 g.

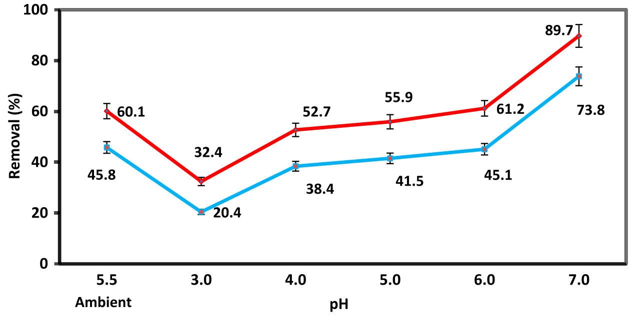

Fig. 6. Effect of pH on Cu(II) removal by Mumong (▬) and Panaga peat (▬): concentration of metal solution: 10.0 mg L^{-1}; volume: 50.0 mL; peat: 0.10 g.

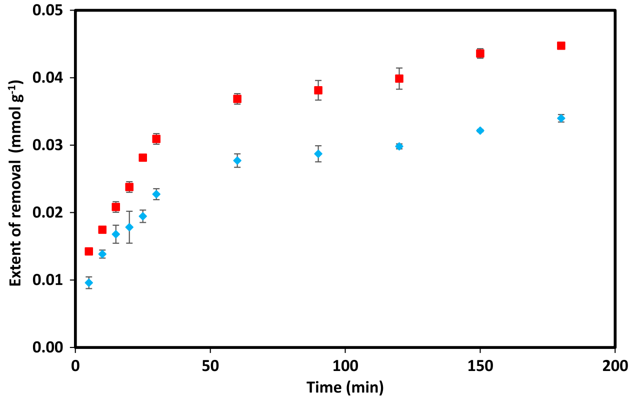

Fig. 7. Variation of the extent of Cu(II) removal in relation to interaction time: Mumong (■) and Panaga (◆). Concentration of metal solution: 10.0 mg L^{-1}; volume: 50.0 mL; peat: 0.10 g.

respectively, and k_1 is the rate constant for adsorption (min^{-1}). The value of k_1 is calculated from the slope of linear plot of $\log(q_e - q_t)$ vs. t.

The rate law of the pseudo-second-order model can be defined as:

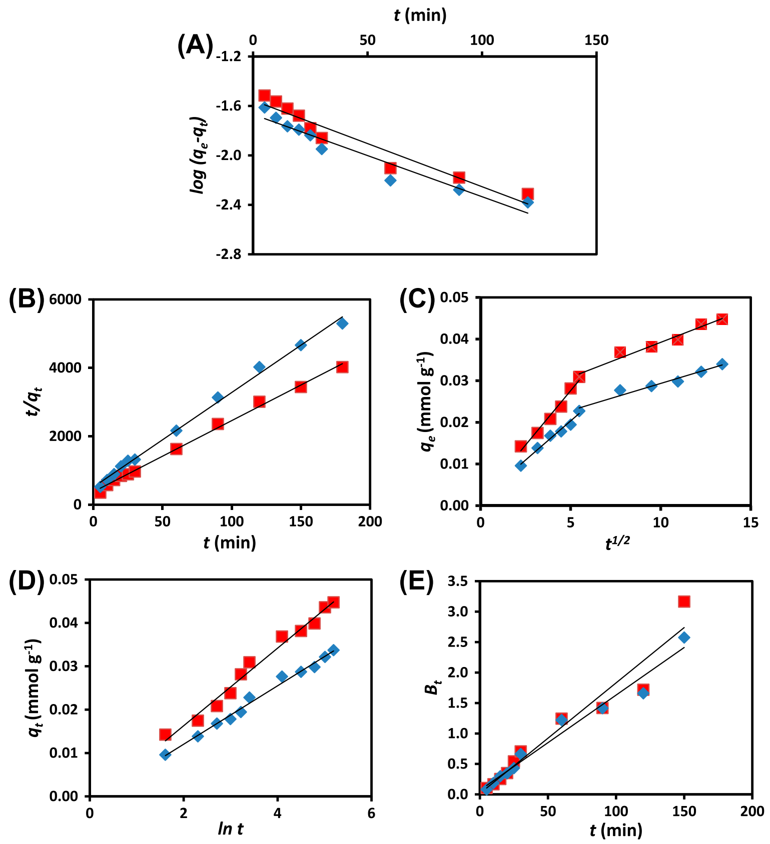

Fig. 8. Kinetics models for Cu(II) removal by Mumong (■) and Panaga (◆): (A) pseudo-first order, (B) pseudo-second order, (C) intraparticle diffusion, (D) Elovich, and (E) Boyd. Concentration of metal solution: 10.0 mg L^{-1}; volume: 50.0 mL; peat: 0.10 g.

$$\frac{1}{q_t} = \frac{1}{k_2 q_e^2} + \frac{1}{q_e} t \tag{4}$$

where q_e (mmol g^{-1}) is the amount adsorbed at equilibrium and k_2 (g $mmol^{-1}$ min^{-1}) is the pseudo-second-order rate constant. The initial adsorption rate h (mmol g^{-1} min^{-1}) at $t \rightarrow 0$ is as follows:

$$h = k_2 q_e^2 \tag{5}$$

The linear plot of t/q_t vs. t gives slope of $1/q_e$ and intercept of $1/k_2 q_e^2$.

The Elovich kinetics model has been applied to adsorption in heterogeneous solution/solid systems. Chien and Clayton [45] simplified the Elovich equation by assuming that $\alpha\beta t >> 1$ and applying the boundary conditions that $q = 0$ at $t = 0$ and $q = q$ at $t = t$, and the equation can then be expressed as follows:

$$q_t = \frac{1}{\beta} \ln(\alpha\beta) + \frac{1}{\beta} \ln t \tag{6}$$

where α (mmol g^{-1} min^{-1}) is the initial sorption rate and β (g $mmol^{-1}$) is related to the extent of surface coverage and activation energy for chemisorption.

The parameters obtained for these models are reported in Table 5. Even though the pseudo-first- and pseudo-second-order models gave high $R^2 > 0.93$ for both peat samples, it is evident from the low χ^2 error values that the adsorption systems under investigation followed the pseudo-second-order mechanism. Further, simulated plots of q_e calculated for both the pseudo-first-order and pseudo-second-order models with experimental values of q_e in Fig. 9 showed that the pseudo-second order gave the closer values to the experimental data further confirming that the adsorption kinetics of Cu(II) on peat follows the pseudo-second-order model. This is also in agreement to previous reports on the adsorption of Cu(II) on peat [36,46]. The pseudo-second-order model assumes that chemisorption is the rate-limiting step involving bonding through sharing or exchange of electrons between adsorbate and adsorbent. The Elovich kinetics model also gave high R^2 values >0.98 suggesting chemisorption of Cu(II) on peat [47].

Table 5
Parameters for kinetics models for adsorption of Cu(II)

Kinetics	Mumong	Panaga
$q_{e,exp}$ (mmol g^{-1})	0.045	0.034
Pseudo-first order		
k_1 (min^{-1})	0.016	0.0154
$q_{e,calc}$ (mmol g^{-1})	0.028	0.021
R^2	0.931	0.931
χ^2	0.185	0.136
Pseudo-second order		
k_2 (g mmol^{-1} min^{-1})	1.153	1.490
h (mmol g^{-1} min^{-1})	0.003	0.002
$q_{e,calc}$ (mmol g^{-1})	0.048	0.036
R^2	0.966	0.996
χ^2	0.001	0.001
Elovich		
a (mmol g^{-1} min^{-1})	0.007	0.005
b (g mmol^{-1})	112.36	147.06
R^2	0.982	0.989
Boyd		
D_i (cm^2 s^{-1}) × 10^{-6}	3.33	2.85
R^2	0.938	0.969

Contribution of diffusion mechanism for the adsorption of Cu(II) on peat samples was evaluated using both the Webber–Morris intaparticle diffusion and Boyd models. If the adsorbate transport is within the pores of the adsorbent, then particle diffusion takes place whereas film diffusion is to the external surface of the adsorbent. The rate constant (k_3) for Weber–Morris intraparticle diffusion model is given as:

$$q_t = k_3 t^{1/2} + C \tag{7}$$

where q_t is the amount adsorbed (mmol g^{-1}) at time t (min), k_3 is the rate constant of the intraparticle diffusion (g mmol^{-1} min^{-1}), and C (mmol g^{-1}) is the constant that depicts the adsorption mechanism. The linear plot of q_t vs. $t^{1/2}$ is used to calculate the parameters of intraparticle diffusion model.

The Boyd's kinetics can be expressed as follows:

$$F = 1 - \frac{6}{\pi^2}\exp(-B_t) \tag{8}$$

and

$$F = \frac{q_t}{q_e} \tag{9}$$

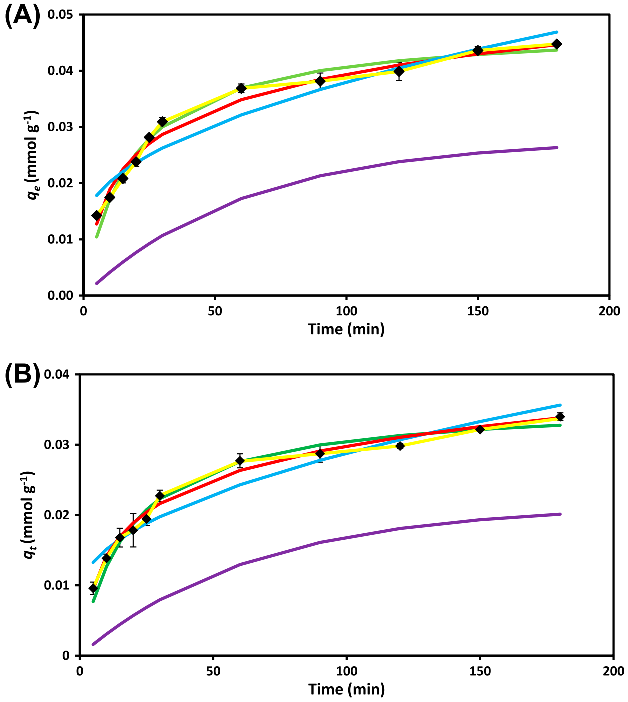

Fig. 9. Simulated plots of experimental and calculated q_t values of Mumong (A) and Panaga (B) peat with various kinetics models; experimental (◆), pseudo-first order (🟪), pseudo-second order (🟩), Elovich (🟥), Boyd (🟨), Weber–Morris intraparticle diffusion (🟦).

where F is the fraction of solute adsorbed at any time (t) and B_t is mathematical function of F.

Rearranging Eq. (15) gives:

$$1 - F = \frac{6}{\pi^2}\exp(-B_t) \tag{10}$$

and

$$B_t = -0.4977 - \ln(1 - F) \tag{11}$$

In this study, linear plots of the Weber–Morris intraparticle diffusion (Fig. 8(C)) and Boyd (Fig. 8(E)) models gave y-intercepts very close to the origin and high R^2 values >0.94 for both the Mumong and Panaga peat samples, clearly indicating that intraparticle diffusion could be the rate-determining step involved.

Peat has a porous structure and this type of adsorbent often results in intraparticle diffusion being the rate-limiting step. Fig. 8(C) shows a multi-linear plot for intraparticle diffusion model, and the parameter values are given in Table 6. A multi-linear nature of

Table 6
Parameters for intraparticle diffusion model for the adsorption of Cu(II)

Cu(II)		C (mmol g^{-1})	k_3 (mmol g^{-1} min$^{-0.5}$)	R^2
Mumong	1st stage	0.002	0.005	0.978
	2nd stage	0.005	0.002	0.969
Panaga	1st stage	0.002	0.004	0.979
	2nd stage	0.016	0.001	0.962

the plot is indicative of the involvement of a few processes. The initial part could be due to rapid boundary layer diffusion and then the gradual adsorption stage followed by the equilibrium stage.

Due to large array of chemical species present in peat which are capable of ion exchange making the adsorption process complex, the adsorption mechanism consists of several steps. The rate-controlling step may be diffusion mass transfer or chemical reaction or a combination of two or three of these processes. Hence, it is concluded that pseudo-second order and the intraparticle diffusion are prevailing mechanisms in the adsorption of Cu(II) ions on selected peat samples. Similar findings have been reported on the adsorption of dyes onto peat where adsorption followed the pseudo-second and Elovich kinetics models [25,46] and intraparticle diffusion [48] could be the rate-determining step.

Reports [32,48–50] as well as FTIR from this study have shown that peat consists of various functional groups such as alcohols, amines, phenolic compounds, and carboxylic acids. It has been suggested that COOH could be responsible for the reaction of divalent metals with humic acid and is one of chelate ring formation involving adjacent aromatic COOH and phenolic OH groups. Ion exchange and single Cu(II) ion interaction with peat as well as copper fixing by complexation have also been suggested [46].

3.7. Isotherm studies

In the present study, the six isotherm models used for explaining the adsorption of metal ions on Mumong and Panaga peat are: Langmuir [51], Freundlich [52], Temkin [53], Dubinin–Radushkevich (D–R) [54], Redlich–Peterson (R–P) [55], and Sips [56]. The Langmuir isotherm, a frequently used isotherm, is based on assumption that monolayer sorption occurs on a homogeneous adsorbent surface of identical sites that are equally available and energetically equivalent and that there is no interaction among adsorbate molecules. It is defined mathematically as:

$$\frac{C_e}{q_e} = \frac{1}{K_L q_{\max}} + \frac{C_e}{q_{\max}} \tag{12}$$

where q_e (mmol g^{-1}) is the amount of adsorbate adsorbed at equilibrium per mass of adsorbent, C_e (mg L^{-1}) is the concentration of adsorbate in aqueous solution at equilibrium, $q_{\max}$ (mmol g^{-1}) is the complete monolayer capacity, and K_L (L mmol^{-1}) is the adsorption equilibrium constant related to energy of adsorption. The monolayer coverage ($q_{\max}$) and K_L of Langmuir isotherm are determined from the slope and intercept of linear plot of C_e/q_e vs. C_e. The affinity between the adsorbate and adsorbent can be predicted using separation factor or dimensionless equilibrium parameter, R_L, which is defined as:

$$R_L = \frac{1}{(1 + K_L C_o)} \tag{13}$$

where K_L is the Langmuir constant and C_o is the initial concentration of metal ions. R_L provides important information on the nature of adsorption, which is stronger for lower R_L values [57]. The value of R_L indicates the type of Langmuir isotherm to be irreversible ($R_L = 0$), favorable ($0 < R_L < 1$), linear ($R_L = 1$), or unfavorable ($R_L > 1$). The R_L is found in the range of 0–1 for concentrations of 5–100 mg L^{-1} Cu(II) which indicates the favorable adsorption (Table 7).

The Freundlich isotherm is based on adsorption on a heterogeneous surface with a non-uniform distribution of heat of adsorption over the surface, whose linear form is as follows:

$$\log q_e = \log K_F + \frac{1}{n} \log C_e \tag{14}$$

where K_F (mmol g^{-1}) and $1/n$ are the Freundlich isotherm constants. K_F and $1/n$ are related to adsorption capacity and adsorption intensity, respectively. This model provides no information on the maximum adsorption capacity ($q_{\max}$) in contrast to Langmuir

Table 7
Separation factor (R_L) for adsorption of Cu(II) on Mumong and Panaga peat

	Initial concentration		
Metal ions	$C_o = 5$ mg L^{-1}	$C_o = 50$ mg L^{-1}	$C_o = 100$ mg L^{-1}
Mumong	0.6	0.1	0.1
Panaga	0.8	0.3	0.2

model [58]. If $n = 1$, the adsorption is linear with adsorption sites homogeneous in energy and no interaction among adsorbed species similar to Langmuir's assumption. If $n < 1$, adsorption is a chemical process, while $n > 1$ indicates a physical process [59]. In this study, n values are greater than unity indicating physisorption [60].

The Temkin isotherm equation assumes that there is a linear decrease rather than logarithmic in the heat of adsorption with coverage as adsorption process progresses. The Temkin isotherm is given as:

$$q_e = B \ln K_T + B \ln C_e \quad \text{and} \quad B = \frac{RT}{b_T} \tag{15}$$

where K_T (L mmol^{-1}) is the equilibrium binding constant corresponding to the maximum binding energy, B is related to the heat of adsorption, and b_T is the variation of adsorption energy (kJ mol^{-1}).

The Dubinin–Radushkevich (D–R) isotherm helps to deduce the characteristic porosity of the adsorbent and the energy of adsorption. It assumes that there is a surface area where the adsorption energy is homogeneous. This approach is usually applied to distinguish the physical and chemical adsorption. The linear form of the D–R isotherm is given in Eq. (16) as:

$$\ln q_e = \ln q_{\max} - B_D \in^2 \quad \text{and} \quad \in = RT \ln\left(1 + \frac{1}{C_e}\right) \tag{16}$$

The energy of adsorption (E) is calculated using Eq. (17) as shown below:

$$E = \frac{1}{\sqrt{2B_D}} \tag{17}$$

The constant $q_{\max}$ (mmol g^{-1}) is the saturation capacity, $\in$ is Polanyi potential and B_D (mol^2 J^{-2}) is a constant related to the mean free energy of adsorption per mole of the adsorbate, and E (kJ mol^{-1}) is the mean free energy of adsorption per molecule of the adsorbate when transferred to the surface of the solid from infinity in solution. If the value of E lies between 8 and 16 kJ mol^{-1}, the adsorption process is a chemisorption, while if $E < 8$ kJ mol^{-1}, it indicates a physical adsorption process [61]. The plot of $\ln q_e$ against $[RT \ln(1 + 1/C_e)]^2$ gives the constants $q_{\max}$ and B_D from the intercept and slope, respectively. In this study, E was found to be 1.26 and 0.39 kJ mol^{-1} for Mumong and Panaga peat, respectively, suggesting that Cu(II) adsorption on peat is likely to be physisorption.

The Sips model is a three-parameter model, considered as a combination of the Langmuir and Freundlich equations, deduced for predicting the heterogeneous adsorption systems. At lower solute concentration, it follows the Freundlich isotherm and thus does not obey Henry's law, while at higher solute concentration, it turns to the Langmuir. The linear form of the Sips isotherm is given in Eq. (18) as:

$$\ln\left(\frac{q_e}{q_{\max} - q_e}\right) = \frac{1}{n} \ln C_e + \ln K_S \tag{18}$$

where K_S (L mmol^{-1}) is the equilibrium constant and n is the Sips model exponent regarded as the heterogeneity factor with values greater than 1 indicating a heterogeneous system and values close to or equal to 1 indicate material with relatively homogenous binding sites [38]. If $n = 1$, the Sips model follows the Langmuir, and if either C_e or K_S approaches 0, it reduces to the Freundlich isotherm. The parameters of the Sips isotherm can be calculated by plotting $\ln [q_e/(q_{\max} - q_e)]$ against $\ln C_e$.

Another three-parameter isotherm model used in this study is the Redlich–Peterson (R–P) model. The R–P isotherm, expressed as Eq. (19), is versatile and can be applied to both homogenous and heterogeneous systems. Its linearized form is as shown in Eq. (20).

$$q_e = \frac{k_R C_e}{1 + a_R C_e^n} \tag{19}$$

Table 8
Isotherm parameters obtained through different adsorption models for the adsorption of Cu(II) on Mumong and Panaga peat

Model	Parameter	Value	
		Mumong peat	Panaga peat
Langmuir	$q_{\max}$ (mmol g^{-1})	0.15	0.21
	$q_{\max}$ (mg g^{-1})	9.5	13.2
	K_L (L mmol^{-1})	0.14	0.04
Freundlich	K_F (mmol g^{-1})	0.25	0.15
	n	3.52	1.72
Temkin	K_T (L mmol^{-1})	4.94	0.46
	b_T (kJ mol^{-1})	107.25	59.70
Dubinin–Radushkevich (D–R)	$q_{\max}$ (mmol g^{-1})	0.12	0.11
	$q_{\max}$ (mg g^{-1})	7.3	7.26
	B (mol^2 J^2)	3.14×10^{-7}	3.34×10^{-6}
	E (kJ mol^{-1})	1.26	0.39
Sips	$q_{\max}$ (mmol g^{-1})	0.26	0.23
	$q_{\max}$ (mg g^{-1})	16.5	14.6
	K_S (L mmol^{-1})	0.18	0.04
	n	2.35	1.11
Redlich–Peterson (R–P)	$q_{\max}$ (mmol g^{-1})	0.06	0.02
	$q_{\max}$ (mg g^{-1})	3.9	1.48
	n	0.81	0.53
	K_R (mmol g^{-1})	0.11	0.02
	a_R (L mmol^{-1})	1.8	0.86

Table 9
Linear regression coefficients and errors for various isotherm models investigated

Model	R^2	HYBRID	EABS	χ^2
Mumong peat				
Langmuir	0.986	0.21	0.09	0.02
Freundlich	0.979	0.04	0.05	0.03
Temkin	0.982	0.02	0.04	0.00
Dubinin–Radushkevich (D–R)	0.744	0.56	0.18	0.05
Sips	0.988	0.02	0.04	0.00
Redlich–Peterson (R–P)	0.999	0.02	0.03	0.00
Panaga peat				
Langmuir	0.975	0.08	0.06	0.01
Freundlich	0.956	0.13	0.08	0.01
Temkin	0.969	0.15	0.08	0.01
Dubinin–Radushkevich (D–R)	0.746	1.09	0.26	0.10
Sips	0.979	0.08	0.06	0.01
Redlich–Peterson (R–P)	0.923	0.12	0,07	0.01

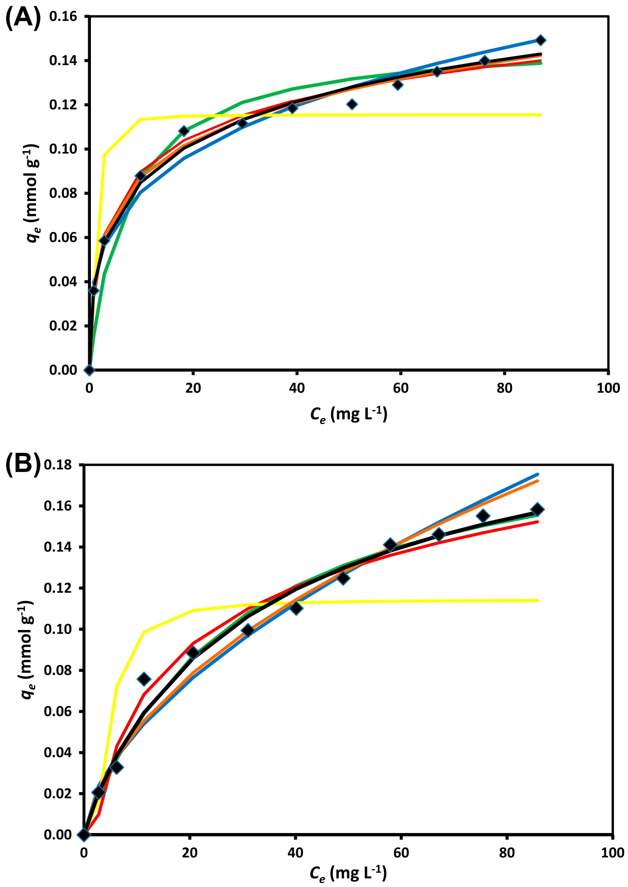

Fig. 10. Different isotherm models for adsorption of Cu(II) onto (A) Mumong and (B) Panaga peat [experiment (♦), Langmuir (🟩), Freundlich (🟦), D–R (🟨), Temkin (🟥), R–P (🟧), Sips (⬛)].

$$\ln\left(k_R \frac{C_e}{q_e} - 1\right) = n \ln C_e + \ln a_R \qquad (20)$$

Table 8 shows the values of parameters obtained for all isotherms models investigated. It can be seen that the D–R isotherm gave the lower R^2 for both the peat samples, clearly indicating that this is an unsuitable model for the adsorption of Cu(II). All the other five isotherm models gave good R^2 (>0.96). In order to determine which of these isotherms is better suited to the adsorption of Cu(II) on peat, three different error analyses (HYBRID, EABS, and χ^2) were performed. Table 9 shows the values of each error function for the isotherm models.

In terms of lowest overall errors, the Sips, Temkin, and R–P provide validity for Mumong peat, while the Langmuir and Sips are good for Panaga peat. In addition, there is a good agreement between $q_{\max}$ values determined for the Langmuir and Sips isotherms for Panaga peat. Further, as the Sips isotherm model can be fitted to both the Mumong and Panaga peat, and it is believed that the Sips equation provides more realistic adsorption capacity than that from the Langmuir equation [30]. Based on the values of regression (R^2) and error functions, the order of the validity of the isotherm models is: R–P ≥ Sips ≈ Temkin > Freundlich > Langmuir > D–R for Mumong and Sips ≥ Langmuir ≈ Temkin > Freundlich ≥ R–P > D–R for Panaga. The maximum adsorption capacities ($q_{\max}$) for Cu(II) peat determined by Sips are 16.5 and 14.6 mg g^{-1} on Mumong and Panaga peat samples, respectively.

Table 10
Comparison of adsorption capacities of different adsorbents

Adsorbent	$q_{\max}$ (mg g^{-1})	Refs.
Mumong peat	16.5	This work
Panaga peat	14.6	This work
Herbaceous peat	4.8	[46]
Irish peat moss	17.6	[47]
Pristine peat	17.8	[36]
Saccharomyces cerevisiae (Baker's yeast)	1.3	[16]
Banana peel	4.8	[17]
Orange peel	3.6	[17]
Kaolinite	10.8	[18]
Tea waste	8.6	[7]
Black carrot residues	8.9	[62]
Coconut tree sawdust	3.9	[63]
Sugarcane bagasse	3.7	[63]

This can be further confirmed with the simulated plot (Fig. 10) comparing the theoretical Langmuir, Freundlich, Temkin, D–R, R–P, and Sips isotherms with the experimental data for the adsorption of Cu (II) onto Mumong and Panaga peat.

3.8. Comparison with other adsorbents

A comparison of the adsorption capacity ($q_{\max}$) of the peat under investigation with other types of peat as well as other adsorbents reported is given in Table 10. When compared to other adsorbents, both peat types used in this study showed higher adsorption capacities. The differences in $q_{\max}$ are due to the nature and properties of each adsorbent, such as chemical structure of the adsorbents and surface area. A comparison with other adsorbents, such as banana peel, orange peel, and tea waste, indicates a high Cu (II) adsorption capacity of the Mumong and Panaga peat.

4. Conclusion

Characterization of peat samples collected from Mumong and Panaga areas in Brunei Darussalam revealed their acidic nature. The H/C ratio is similar for both peat types suggesting the similar degree of aromatic components present in both, and further, Panaga peat shows a significantly lower C/N ratio suggesting it more decomposed. SEM images showed porous structure and the presence of elements is confirmed through XRF analysis. High value of ash indicates high amounts of minerals in peat. In addition, thermogravimetric analysis indicates that the Mumong peat is more thermally stable than the Panaga peat. The adsorption isotherms and the kinetics studies revealed strong adsorption behavior of peat toward Cu(II). The equilibrium isotherm data analyzed using the Langmuir, Freundlich, Temkin, Dubbinin–Radushkevich, Redlich–Peterson, and Sips isotherm models demonstrate that the Sips isotherm provided the best correlation coefficient and lowest error values for adsorption of Cu(II) on both peat types. Reasonably high adsorption capacity of 16.5 and 14.6 mg g^{-1}, as compared to other reported adsorbents, was obtained for the Mumong and Panaga peat, respectively, indicating the Bruneian peat has promising use as an adsorbent in wastewater treatment containing Cu(II) ions. The kinetics of peat interactions is very complex, and different mechanisms of interactions based on the pseudo-second-order and intraparticle diffusion processes would play a role in the adsorption of Cu(II). It could be concluded that the Mumong and Panga peat have a potential to be used as low-cost natural and abundant source for the removal of Cu(II).

Acknowledgments

The authors would like to thank the Government of Brunei Darussalam and the Universiti Brunei Darussalam (UBD) for their financial support. The authors are also grateful to the Energy Research Group (CAMES) and the Department of Biology at UBD for the use of XRF and SEM, respectively.

References

[1] S.E. Page, J.O. Rieley, C.J. Banks CJ, Global and regional importance of the tropical peatland carbon pool, Global Change Biol. 17 (2011) 798–818.
[2] L. Gandois, R. Teisserenc, A.R. Cobb, H.I. Chieng, L.B.L. Lim, A.S. Kamariah, A. Hoyt, C.F. Harvey, Origin, composition and transformation of dissolved organic matter in tropical peatlands, Geochim. Cosmochim. Acta 137 (2014) 35–47.
[3] D. Cohen, M.S. Rollin, W.M. Zunic, Effects of chemical and physical differences in peats on their ability to extract hydrocarbons from water, Water Resour. 25 (1991) 1047–1060.
[4] M. Corley, M. Rodgers, J. Mulqueen, E. Clifford, The performance of fibrous peat biofilters in treating domestic strength wastewater, J. Environ. Sci. Health, Part A 41 (2006) 811–824.
[5] S. Suni, A.L. Kosunen, M. Hautala, A. Pasila, M. Tomantschuk, Use of by-product of peat excavation. Cotton grass fibre, as a sorbent for oil spills, Mar. Pollut. Bull. 49 (2006) 916–921.
[6] T. Viraraghavan, S.R. Kikkeri, Peat filtration of food-processing wastewaters, Biological Wastes 26 (1988) 151–155.
[7] S. Cay, A. Uyanik, A. Ozasik, Single and binary component adsorption of copper(II) and cadmium(II) from aqueous solutions using tea-industry waste, Sep. Purif. Technol. 38 (2004) 273–280.
[8] S. Mehdizadeh, S. Sadjadi, S.J. Ahmadi, M. Outokesh, Removal of heavy metals from aqueous solution using platinum nanoparticles/Zeolite-4A, J. Environ. Health Sci. Eng. 12 (2014), doi: 10.1186/2052-336X-12-7.
[9] M.K. Dahri, M.R.R. Kooh, L.B.L. Lim, Removal of methyl violet 2B from aqueous solution using *Casuarina equisetifolia* needle, ISRN Environ. Chem. 2013 (2013) Article ID 619819. Available from: <http://dx.doi.org/10.1155/2013/619819>.
[10] L.B.L. Lim, N. Priyantha, C.M. Chan, D. Matassan, H.I. Chieng, M.R.R. Kooh, Adsorption behavior of methyl violet 2B using duckweed: Equilibrium and kinetics studies, Arab. J. Sci. Eng. 39 (2014) 6757–6765.
[11] N. Priyantha, L.B.L. Lim, D.T.B. Tennakoon, N.H.M. Mansor, M.K. Dahri, H.I. Chieng, Breadfruit (*Artocarpus altilis*) waste for bioremediation of Cu(II) and Cd (II) ions from aqueous medium, Ceylon J. Sci. (Phys. Sci.) 17 (2013) 19–29.

[12] M.K. Dahri, M.R.R. Kooh, L.B.L. Lim, Water remediation using low cost adsorbent walnut shell for removal of malachite green: Equilibrium, kinetics, thermodynamic and regeneration studies, J. Environ. Chem. Eng. 2 (2014) 1434–1444.

[13] B.A. Fil, R. Boncukcuoğlu, A.E. Yilmaz, S. Bayar, Adsorption of Ni(II) on ion exchange resin: Kinetics, equilibrium and thermodynamic studies, Korean J. Chem. Eng. 29 (2012) 1232–1238.

[14] B.A. Fil, R. Boncukcuoğlu, A.E. Yilmaz, S. Bayar, Adsorption kinetics and isotherms for the removal of zinc ions from aqueous solution by an ion-exchange resin, J. Chem. Soc. Pakistan 34 (2012) 841–848.

[15] B.A. Fil, A.E. Yilmaz, R. Boncukcuoğlu, S. Bayar, Removal of divalent heavy metal ions from aqueous solutions by Dowex HCR-S synthetic resin, Bulgarian Chem. Commun. 44 (2012) 201–207.

[16] M.H. Saleem, F.A. Hanan, A.M. Ehab, F.M. Mohammad, Optimization of cadmium, zinc and copper biosorption in an aqueous solution by Saccharomyces cerevisiae, J. Am. Sci. 6 (2010) 597–604.

[17] G. Annadural, R.S. Juang, D.J. Lee, Adsorption of heavy metals from water using banana and orange peel, Water Sci. Technol. 47 (2002) 185–190.

[18] Ö. Yavuz, Y. Altunkaynak, F. Güzel, Removal of copper, nickel, cobalt and manganese from aqueous solution by kaolinite, Water Res. 37 (2003) 948–952.

[19] T. Zehra, L.B.L. Lim, N. Priyantha, D.T.B. Tennakoon, Sorption characteristics of peat of Brunei Darussalam. II: Interaction of aqueous copper(II) species with raw and processed peat, J. Ecotechnol. Res. 17 (2013) 45–49.

[20] S.R. Shukla, R.S. Pai, Adsorption of Cu(II), Ni(II) and Zn(II) on dye loaded groundnut shells and sawdust, Sep. Purif. Technol. 43 (2005) 1–8.

[21] E. Pehlivan, S. Cetin, B.H. Yanik, Equilibrium studies for the sorption of zinc and copper from aqueous solutions using sugar beet pulp and fly ash, J. Hazard. Mater. 135 (2006) 193–199.

[22] J.-M. Liu, S.T. Lau, H.L.W. Chan, C.L. Choy, J. Zhou, A Monte Carlo simulation on domain pattern and ferroelectric behaviors of relaxor ferroelectrics, J. Mater. Sci. 41 (2006) 163–175.

[23] S. Sabiham, Studies on peat in the coastal plains of Sumatra and Borneo, Southeast Asian Stud. 27 (1989) 339–351.

[24] S.E. Page, J.O. Rieley, R. Wüst, Lowland tropical peatlands of Southeast Asia, Dev. Earth Surf. Process. 9 (2006) 145–172.

[25] T. Zehra, N. Priyantha, L.B.L. Lim, Sorption characteristics of peat of Brunei Darussalam V: Removal of Congo red dye from aqueous solution by peat, Desalin. Water Treat. 54 (2015) 2592–2600.

[26] C.M. Yule, Loss of biodiversity and ecosystem functioning in Indo-Malayan peat swamp forests, Biodivers. Conserv. 19 (2010) 393–409.

[27] L.B.L. Lim, N. Priyantha, D.T.B. Tennakoon, C.H. Ing, C. Bandara, Sorption characteristics of peat of Brunei Darussalam I: Characterization of peat and adsorption equilibrium studies of methylene blue–peat interactions, Ceylon J. Sci. (Phys. Sci.) 17 (2013) 41–51.

[28] P. Kuhry, D.H. Vitt, Fossil carbon/nitrogen ratios as a measure of peat decomposition, Ecology 77 (1996) 271–275.

[29] L. Djurdjević, A. Dinić, M. Mitrović, P. Pavlović, V. Tešević, Phenolic acids distribution in a peat of the relict community with Serbian spruce in the Tara Mt. forest reserve (Serbia), Eur. J. Soil Biol. 39 (2003) 97–103.

[30] L. Gandois, A.R. Cobb, I.C. Hei, L.B.L. Lim, K. Salim, C.F. Harvey, Impact of deforestation on solid and dissolved organic matter characteristics of tropical peat forests: implications for carbon release, Biogeochemistry 114 (2013) 183–199.

[31] A. Usup, Y. Hashimoto, H. Takahashi, H. Hayasaka, Combustion and thermal characteristics of peat fire in tropical peatland in Central Kalimantan, Indonesia, Topics 14 (2004) 1–19.

[32] T. Zehra, L.B.L. Lim, N. Priyantha, Removal behavior of peat collected from Brunei Darussalam for Pb(II) ions from aqueous solution: Equilibrium isotherm, thermodynamics, kinetics and regeneration studies, Environ. Earth Sci. 74 (2015) 2541–2551.

[33] L.B.L. Lim, N. Priyantha, D.T.B. Tennakoon, T. Zehra, Sorption characteristics of peat of Brunei Darussalam II: Interaction of aqueous copper(II) species with raw and processed peat, J. Ecotechnol. Res. 17 (2013) 45–49.

[34] L.B.L. Lim, N. Priyantha, D.T.B. Tennakoon, N.K.M. Mansor, M.H. Dahri, H.I. Chieng, Breadfruit (*Artocarpus altilis*) waste for bioremediation of Cu(II) and Cd(II) ions from aqueous medium, Ceylon J. Sci. (Phys. Sci.) 17 (2013) 19–29.

[35] C.R. Wang, X. Ren, W.-X. Li, Z.-F. Hou, C. Ke, Q. Geng, Adsorption of zinc and copper heavy metal ions from smelting wastewater using modified lava particles, Pol. J. Environ. Stud. 22 (2013) 1863–1869.

[36] H.I. Chieng, L.B.L. Lim, N. Priyantha, Adsorption of copper(II) ions by peat from pristine and disturbed sites: Equilibrium, thermodynamics and kinetics study, J. Appl. Sci. Environ. Sanit. 8 (2013) 303–312.

[37] L.B.L. Lim, N. Priyantha, D.T.B. Tennakoon, M.K. Dahri, Biosorption of cadmium(II) and copper(II) ions from aqueous solution by core of *Artocarpus odoratissimus*, Environ. Sci. Pollut. Res. 19 (2012) 3250–3256.

[38] M. Doğan, Y. Özdemir, M. Alkan, Adsorption kinetics and mechanism of cationic methyl violet and methylene blue dyes onto sepiolite, Dyes Pigm. 75 (2007) 701–713.

[39] Y. Wu, S. Zhang, X. Guo, H. Huang, Adsorption of chromium(III) on lignin, Bioresour. Technol. 99 (2008) 7709–7715.

[40] S. Lagergren, Zur theorie der sogenannten adsorption gelöster stoffe (About the theory of so-called adsorption of soluble substances), Kungliga. Svenska. Vetenskapsakademiens. Handlingar. 28 (1898) 1–39.

[41] Y.S. Ho, G. McKay, Sorption of dye from aqueous solution by peat, Chem. Eng. J. 70 (1998) 115–124.

[42] R.-S. Juang, M.L. Chen, Application of the Elovich equation to the kinetics of metal sorption with solvent-impregnated resins, Ind. Eng. Chem. Res. 36 (1997) 813–820.

[43] G.E. Boyd, A.W. Adamson, L.S. Myers, The exchange adsorption of ions from aqueous solutions by organic zeolites. II. kinetics 1, J. Am. Chem. Soc. 69 (1947) 2836–2848.

[44] W.J. Weber, J.C. Morris, Kinetics of adsorption on carbon from solution, J. Sanit. Eng. Div. 89 (1963) 31–60.

[45] S.H. Chien, W.R. Clayton, Application of Elovich equation to the kinetics of phosphate release and sorption in soils1, Soil Sci. Soc. Am. J. 44 (1980) 265–268.

[46] Y.S. Ho, G. McKay, Application of kinetic models to the sorption of copper(II) on to peat, Adsorpt. Sci. Technol. 20 (2002) 797–815.

[47] C. Aharoni, M. Ungarish, Kinetics of activated chemisorption. Part 1.—The non-elovichian part of the isotherm, J. Chem. Soc., Faraday Trans. 72 (1976) 400–408.

[48] H.I. Chieng, T. Zehra, L.B.L. Lim, N. Priyantha, D.T.B. Tennakoon, Sorption characteristics of peat of Brunei Darussalam IV: Equilibrium, thermodynamics and kinetics of adsorption of methylene blue and malachite green dyes from aqueous solution, Environ. Earth Sci. 72 (2014) 2263–2277.

[49] H.I. Chieng, L.B.L. Lim, N. Priyantha, N. Priyantha, Sorption characteristics of peat from Brunei Darussalam for the removal of rhodamine B dye from aqueous solution: Adsorption isotherms, thermodynamics, kinetics and regeneration studies, Desalin. Water Treat. 55 (2015) 664–677.

[50] H.I. Chieng, N. Priyantha, L.B.L. Lim, Effective adsorption of toxic brilliant green from aqueous solution using peat of Brunei Darussalam: Isotherms, thermodynamics, kinetics and regeneration studies, RSC Adv. 5 (2015) 34603–34615.

[51] I. Langmuir, The constitution and fundamental properties of solids and liquids. Part I. Solids, J. Am. Chem. Soc. 38 (1916) 2221–2295.

[52] H.M.F. Freundlich, Uber die adsorption in losungen (adsorption in solution), J. Phys. Chem. 57 (1906) 384–470.

[53] M.I. Temkin, V. Pyzhev, Kinetics of ammonia synthesis on promoted iron catalyst, Acta Phys. Chim. URSS. 12 (1940) 327–356.

[54] M.M. Dubinin, L.V. Radushkevich, The equation of the characteristic curve of the activated charcoal, Proc. Acad. Sci. USSR Phys. Chem. Sec. 55 (1947) 331–337.

[55] O. Redlich, D.L. Peterson, A useful adsorption isotherm, J. Phys. Chem. 63 (1959) 1024–1024.

[56] R. Sips, On the structure of a catalyst surface, J. Chem. Phys. 16 (1948) 490–495.

[57] M. Belhachemi, F. Addoun, Comparative adsorption isotherms and modeling of methylene blue onto activated carbons, Appl. Water Sci. 1 (2011) 111–117.

[58] Z. Aksu, E. Balibek, Chromium(VI) biosorption by dried *Rhizopus arrhizus*: Effect of salt (NaCl) concentration on equilibrium and kinetic parameters, J. Hazard. Mater. 145 (2007) 210–220.

[59] A.M. Farha, A.H. Al-Dujaili, A.M. Awwad, Equilibrium and kinetic studies of cadmium(II) and lead(II) ions biosorption onto Ficuscarcia leaves, Int. J. Ind. Chem. 4 (2013), doi: 10.1186/2228-5547-4-24.

[60] J.Q. Jiang, C. Cooper, S. Ouki, Comparison of modified montmorillonite adsorbents, Chemosphere 47 (2002) 711–716.

[61] J. Liu, X. Wang, Novel Silica-based hybrid adsorbents: Lead(II) adsorption isotherms, Sci. World J. (2013), doi: 10.1155/2013/897159.

[62] F. Guzel, H. Yakut, G. Topal, Determination of kinetic and equilibrium parameters of the batch adsorption of Mn(II), Co(II), Ni(II) and Cu(II) from aqueous solution by black carrot (*Daucus carota* L.) residues, J. Hazard. Mater. 153 (2008) 1257–1287.

[63] W.P. Putra, A. Kamari, S.N.M. Yusoff, C.F. Ishak, A. Mohamed, N. Hashim, I.M. Isa, Biosorption of Cu(II), Pb(II) and Zn(II) ions from aqueous solutions using selected waste materials: Adsorption and characterisation studies, J. Encapsulation Adsorpt. Sci. 4 (2014) 25–35.